Application of a handheld X-ray fluorescence spectrometer for real-time, high-density quantitative analysis of drilled igneous rocks and sediments during IODP Expedition 352

J.G. Ryan[1], J.W. Shervais[2], Y. Li[3], M.K. Reagan[4], H.Y. Li[5], D. Heaton[6], M. Godard[7], M. Kirchenbaur[8], S. Whattam[9], J.A. Pearce[10], T. Chapman[11], W. Nelson[12], J. Prytulak[13], K. Shimizu[14], K. Petronotis[15], and the IODP Expedition 352 Scientific Team[16]

[1]{School of Geosciences, University of South Florida, Tampa, FL, USA}
[2]{Geology, Utah State University, USA}
[3]{Institute of Geology, Chinese Academy of Geological Sciences, Beijing, China}
[4]{Dept. Earth and Environmental Sciences, University of Iowa, Iowa City, USA}
[5]{State Key Laboratory of Isotope Geochemistry, Guangzhou Institute of Geochemistry, Chinese Academy Science, Guangzhou 510640, China}
[6]{College of Earth, Ocean and Atmospheric Sciences, Oregon State Univ., Corvallis, OR}
[7]{Geosciences, Universite Montpellier II, Montpellier, France}
[8]{Geologische Inst., Universitat Koln, Koln, Germany}
[9]{Dept. Earth and Environmental Sciences, Korea University, Republic of Korea}
[10]{Earth and Ocean Sciences, Cardiff University, UK}
[11]{School of Geosciences, University of Sydney, Australia}
[12]{Physics, Astronomy, Geosciences; Towson University, MD, USA}
[13]{Earth Sciences and Engineering, Imperial College, UK}
[14]{International Ocean Discovery Program, College Station, TX, USA}
[15] {Kochi Core Center, Kochi University, Japan}
[16]{R. Almeev, A. Avery, C. Carvallo, G. Christeson, E. Ferre, W. Kurz, S. Kutterolf, K. Michibayashi, S. Morgan, M. Python A. Robertson, W. Sager, T. Sakuyama; see http://iodp.tamu.edu/scienceops/precruise/izuboninforearc/participants.html for affiliations}

Correspondence to: J. G. Ryan (ryan@mail.usf.edu)

Abstract

Handheld energy dispersive portable X-ray spectrometers (pXRF) are generally designed and used for qualitative survey applications. We developed shipboard quantitative analysis protocols for pXRF and employed the instrument to make over 2000 individual abundance measurements for a selection of major and trace elements on over 1200 meters of recovered core during the eight weeks of the International Ocean Discovery Program (IODP) Expedition 352 to the Izu-Bonin forearc. pXRF analytical performance, accuracy and precision were found to be the same on powdered rock samples and on freshly cut rock surfaces, and sample

results were similar within error to measurements made via shipboard ICP-OES analysis save at low abundance levels for a few elements. Instrument performance was optimal for elements between Z=19 and Z=40, and the system yielded reproducible data for K, Ca, Ti, V, Cr, Mn, Fe, Cu, Zn, Rb, Sr, and Zr on both powdered samples and rock surfaces. Working curves developed via pXRF measurement of a suite of geologic standard reference materials and well-characterized lavas permitted accurate quantitative measurements for many of the examined elements on both sample powders and rock surfaces. Although pXRF has been sporadically employed on previous cruises, Expedition 352 is the first time a detailed, high-density chemostratigraphy of recovered core samples was collected using pXRF measurements of rock core surfaces. These high-resolution data allowed the recognition of chemically distinct eruptive units in near real-time. The rapid identification of geochemical trends vastly improved our selection of samples for shipboard and shore-based analysis, permitted a more comprehensive interpretation of our Expedition results, and provided key decision-making information for drilling operations.

1 Introduction

A significant challenge faced in oceanic drilling expeditions is the ability to perform basic chemical characterization of recovered materials in a timely enough fashion to monitor rock type and downhole stratigraphic information during coring. While it is established practice to cut thin sections and conduct bulk chemical analysis of recovered samples as they are collected, these procedures typically require several days to complete. This can pose significant challenges during hard-rock drilling, because recovery in igneous rocks is often poor, and volcanic igneous rocks in particular may not exhibit clear mineralogical, textural, or other macroscopic characteristics that permit ready classification.

International Ocean Discovery Program (IODP) Expedition 352 aimed to drill a complete volcanic reference section in the Izu-Bonin outer forearc (Reagan et al., 2015). Over 1200 m of basaltic and boninitic lavas were drilled, with limited to poor recovery (~12% in basalts; ~30% in boninites; see Reagan, et al 2015). While variations in eruptive style and alteration were at times evident, some recovered samples were phenocryst-poor and uniform in appearance. Thin sectioning of samples and ICP-OES measurements on the *JOIDES Resolution* (*JR*) permitted the characterization of recovered samples for phenocryst assemblages as well as major oxides and selected high-abundance trace elements. However,

poor correlation between phenocryst and compositional variations, the substantial time lag between sample recovery and geochemical analysis (~1 week to powder, digest, and analyze samples via ICP-OES), and limits on the number of samples that could feasibly be processed and analyzed on the ship severely impact the ability to track volcanic rock compositions downhole in real time. Such knowledge of downhole variation is often crucial for operational decision-making.

Seeking a better means for rapid and quantitative chemical characterization of drill core, the Expedition 352 geochemistry and petrology scientists turned to a handheld portable X-ray fluorescence spectrometer (pXRF), which was available onboard for the expedition, but had not been previously employed for real time hard-rock core characterization. pXRF has been used widely to identify contaminants in soils, to assay the provenance of geo-archaeological materials, and to characterize cultural materials in archaeology (see Potts and West 2008; Zhu et al 2011; Weindorf et al 2012; Conrey et al 2014; Hu et al 2014; Swanhart et al 2014; Tykot, 2016, among others). The uses of pXRF and related methods such as X-ray core scanning in marine geological applications have mostly focused upon the characterization of recovered submarine sediments (e.g., Wien et al 2005; Kido et al 2006; Jan Weltje and Tjallinge, 2008; Lowemark et al 2011; Hennekam and deLange, 2012; Liang et al 2012; Rowe et al 2012). Aside from offering quick measurements (1-2 minutes for fresh sample surfaces and/or powders), we found that the method provided quantitative results at reasonable precision and accuracy for a selection of useful major and trace elements, which permitted the rapid characterization of recovered core samples, as well as straightforward correlations with and confirmations of ICP-OES sample powder results.

2 Methods

2.1 Instrumentation

The shipboard pXRF available on the *JOIDES Resolution* was a Fisher Niton GOLDD+ XL3t handheld instrument, and included sample holders for both round mounts and larger rock pieces (Figure 1). An additional shielded mounting system had been constructed by IODP for pXRF use on larger sections of core. The instrument had been tested to a very limited degree on previous Expeditions (330, 335, 345, 350; see "XRF" in Teagle et al, 2012; also Koppers et al 2012; Gillis et al 2014). The Niton GOLDD+ XL3t is a self-contained energy-dispersive XRF survey instrument with a variable intensity X-ray source (6-50 kV, 0-200 μA Ag anode) and a proprietary GOLDD (Geometrically Optimized Large Area Drift

Detector) detection system that is rated by the manufacturer for low detection limit, high-precision measurement of 30+ elements, though a helium purge is required to obtain results on lower atomic number species (Thermo Scientific, 2016). The instrument includes data correction packages tailored to a variety of applications (metals, plastics, soils and minerals, and consumer goods), and reads out concentration results for each measurement, simplifying data reduction and interpretation. In terms of the specifics of the X-ray technology, the Niton GOLDD+ XL3t instrument differs markedly from wavelength-dispersive XRF instruments that had been used on the *JOIDES Resolution* in the past (see Christie et al, 2001 as an example), especially in that extensive sample preparation is not required. The X-ray analysis strategies of this instrument are more sophisticated than either the tabletop EDS-XRF system employed at sea by Wien et al (2005), or than X-ray core scanners (e.g., Jan Weltje and Tjallinge, 2008; Lowemark et al 2011). It is more directly comparable to the handheld portable XRF instruments described by Weindorf et al (2012) and Rowe et al (2012), albeit with a newer generation detection system and data correction and processing protocols. On Expedition 352, we utilized its "Soils" protocol within the "Soils and Minerals" submenu, as this protocol, which permits calibration on a large number of elements, provided the most reliable concentration results. The Soils protocol is designed to make measurements per US EPA Method 6200 (Thermo Fisher, 2010; USEPA, 2007). The instrument utilizes several excitation filters that optimize instrument sensitivity for measuring elements in four different X-ray energy ranges: the "light" range (for low atomic number elements such as Si, Al and Mg); the "Low" range (which optimizes for Cr, V, Ti, Sc, Ca, K, and S); the "Main" range (optimized for Mo, Zr, Sr, U, Rb, Th, Pb, Au, Se, As, Hg, Zn, W, Cu, Ni, Co, Fe, and Mn); and the "High" range (optimized for Ba, Cs, Te, Sb, Sn, Cd, Ag, and Pd). The Soils protocol applies a modified Compton normalization method for calibration, (i.e., calibration is based on the measurement of a single specific reference sample, recommended in the user manual as the CCRMP TILL-4: Thermo Fisher, 2010; CCRMP, 1995: Table 1). This initial calibration was completed at the factory before the Expedition. "Light" range species can only be measured with a helium purge, which was not available on the ship. Elements in the "High" energy range did not provide reliable results, as most were below their practical detection limits in our samples. "Main" and "Low" energy range species, however, yielded results that were sufficiently precise and accurate for a number of elements when concentrations were above instrument detection limits.

2.2 Elements Detected, Correlation and Accuracy

The elements found to be reliably above instrument detection limits in Expedition 352 materials were Fe, Ca, Mn, Ti, K, Sr, Zr, Cu, Zn, V, and Cr. Ni was above detection limits in our highest-concentration reference materials, like ultramafic rock samples (e.g., USGS Reference material DTS-1 or Geological Survey of Japan reference material JP-1), as well as in some of the boninitic igneous rocks examined during Expedition 352. However it was too close to the pXRF detection limit in many of the other standard reference materials available onboard to develop reasonable working curves (Ni reported level of detection = 25 ppm: Teagle et al 2012; Table 2). Scandium was consistently above detection limits, but yielded scattered and un-correlated results that were 3–10 times actual abundances based on reference materials. Thus, Sc and Ni were therefore not measured by pXRF during Expedition 352.

Correlation curves developed for Fe, Ca, Mn, Ti, K, Sr, Zr, Cu, Zn, V, and Cr (i.e., plots of pXRF abundances as per the soils correction protocol versus reported consensus values for reference materials: Table 3; Figure 2) were of varying quality, but many yielded correlation coefficients (r values) of 0.95 or better, indicating high consistency in instrument performance over a range of concentrations. Y-intercept values were significantly offset from the origin for several of the higher abundance elements (Figure 2), in particular Fe. It is probable that this is an effect of the Compton normalization strategy, as Compton normalization can be problematic for elements that show a wide range in abundances, and/or are substantially higher than the values of the standard used (Thermo Fisher 2010), though it may also reflect differences sample matrices (i.e., basaltic/boninitic and ultramafic rocks rich in Fe, Ca, and Mg, vs. glacial till (Table 1)). In addition, the Compton scattered tube line is less effective at estimating mass absorption below the Fe absorption edge, which leads to non-linear response (Reynolds 1963). In the case of iron, the resultant working curve had a high r value, with a negative y intercept of >2% wt; for Ca, the y intercept of the working curve was also negative, but consistently within <0.5% wt. of the origin, so this effect appeared to be less of a concern. Our correlation curve for vanadium had a low r value (due at least in part to low-precision V concentration data for some of the reference materials available on the ship), but pXRF results for V were found to be highly reproducible and at expected abundance levels for the samples examined during Expedition 352, suggesting that for V the pXRF was at least producing an internally consistent data set.

In general, decisions to accept pXRF results for a particular element were based on the correlation curve quality of fit (r values of 0.95 or better), slopes approximating 1.0 (0.9–1.1),

and *y*-intercepts approaching the origin within analytical uncertainties. Data for elements with correlation curves showing substantial offsets in their *y*-intercepts and for elements with correlation curve *r* values of <0.95 were generally not utilized in our interpretations. For the remaining elements, the correlation curves in Figure 2 became the basis for working curves to calculate accurate elemental concentrations. These curves were reliable over the concentration ranges constrained by our reference materials.

2.43 Calibration and use on sample powders and rock surfaces

Working curves for the different elements measured by pXRF were produced using powder mounts of international reference standards (BHVO-2; BCR-2, JB-2, JB-3, AGV-1, MRG-1, JP-1, and DTS-1: Table 1). Additionally, we made use of several previously analyzed Chichijima Island boninite samples (J. Pearce, pers. comm., 2014; Table 1) to provide additional calibration data for boninites, which have unusual compositional profiles. The standards correlation data were evaluated with Microsoft Excel using the LINEST function to produce slope and intercept values (see Figure 2 for the shipboard working curve calculations) that were used to correct the readout concentration data from the instrument relative to accepted standard values, and a correction algorithm was developed for each analyzed element as part of a single data correction spreadsheet. Newly collected pXRF data from rock cores or powders on the ship were all corrected via this approach before their final tabulation and use in the geochemical analysis of recovered materials.

Powdered samples were prepared for analysis using re-usable plastic powder mount assemblies. These sample mounts were designed to fit in the sample holder system provided with the instrument (Figure 1), and yielded consistent results on repeated analysis (i.e., Table 3). Mounts of our pXRF calibration standards were maintained and periodically re-measured during the Expedition, while mounts of powdered unknowns were prepared, measured and disassembled, with the mounts recycled for use as needed.

2.4 Measurement protocols and performance tests on Expedition 352 recovered materials

pXRF measurements on unknowns (sample powders or rock surfaces) were 60 seconds each on the Low, Main, and High range filter elements. Longer count times were possible, and as with any X-ray analysis system longer counting times served to improve overall

precision. However, given that our results were sufficiently reproducible at 60 seconds we chose not to measure for longer periods. Typically three measurements across all three ranges were averaged as a single determination on powdered samples. For rock surfaces three or more measurements at several different positions on the sample constituted a single analysis.

The long-term reproducibility of the pXRF instrument was tracked through a month of its use on the ship through repeated analyses of the USGS reference material BHVO-2 (Table 3). Variability in pXRF results over time was within the instrument's reported measurement uncertainties for all the elements analyzed (Table 3), with no evidence for signal drift over the course of our usage. The accuracy of data for Fe and V were poor, for reasons noted above; issues with the accuracy of Cr data at the abundance levels for BHVO-2 are discussed below.

To assay the performance of the shipboard pXRF instrument on the different kinds of sample materials we encountered on Expedition 352, we conducted tests comparing results on rocks versus powdered samples, and on rock surfaces.

To test the pXRF performance on rock samples as compared to sample powders, we measured with the pXRF a selection of basaltic sample powders from Hole U1440B that had been prepared for ICP-OES analysis and compared these data to measurements on the fresh cut surfaces of thin section billets taken adjacent to each sampling site. The powdered samples were intentionally selected from large, homogeneous core sections, and these became "POOL" samples on which all shipboard scientists would collect data (e.g., Reagan et al 2015). A thin section billet was taken from the same cut core segment for each of the "POOL" samples to provide petrographic context. Comparisons between pXRF analyses on these powders and thin section billets are illustrated in Figure 3.

Possible outcomes for this kind of comparison would be broad abundance similarities between the powders and billets, or potentially significant variability resulting from mineralogical variations in the rock samples and/or differences in packing density of particles in powdered samples with respect to solid rock. Another important concern regarding data quality would be any evidence of systematic differences in abundance levels for all or some elements that might indicate differences in the pXRF response on powders versus rocks. We found good correlations between pXRF data for un-oxidized "POOL" sample powders and the corresponding thin section billets from Hole U1440B for those elements that were not strongly affected by secondary alteration processes, with variability that was at or within the measurement uncertainties of the elements examined (Figure 3). The elements analyzed that were more sensitive to alteration effects (K, Sr, and to a lesser extent Ca) show greater

variability, though even in the case of K, which shows the greatest scatter, most samples are within error of a 1:1 relationship. For these elements, inhomogeneous distribution in secondary minerals may be producing some local variability, but this effect is not evident for the more immobile elements we measured. There was no obvious evidence for performance differences related to material preparation. The pXRF appears to provide comparable results for the selected elements on both powdered and solid-rock versions of what was approximately the same sample material. Thus, for the relatively uniform, aphanitic volcanic rocks encountered in Hole U1440B and at the other Expedition 352 drilling locations, direct pXRF measurements of rock surfaces yielded data that could be directly compared to data derived from powdered samples.

A significant concern with the quantitative analytical use of the pXRF is the degree to which within-sample compositional variability might complicate the interpretation of measured results. To evaluate this issue, a thin section billet from a previously analyzed basaltic rock sample from our field area (Sample 1090-20; Reagan et al., 2010), comparable compositionally and texturally to Site U1440B recovered basalts, was analyzed multiple times at a variety of different positions on the sample's cut surface. The results of this test are presented in Table 4. The standard deviation of our analyses varied by element as a function of overall abundance level and instrument performance, with some elements showing as little as 3% overall variation. The resulting analyses were largely comparable to the published results for this sample (e.g., Reagan et al 2010), as constrained by the calibration of the instrument and our approach (see Figure 2 and discussion below), indicating that for the fine grained igneous rocks recovered at Site U1440 and similar igneous rock samples from the other Expedition 352 sites, within-sample variability is not a significant concern.

2.5: Comparisons of pXRF performance to other analytical methods

On the ship we made comparisons of our pXRF results with measurements made using the shipboard ICP-OES (Reagan et al 2015). While ICP-OES measurements were conducted on solutions made via lithium borate fusions of sample powder aliquots, which had been heated in a muffle furnace for Loss on Ignition determinations, pXRF measurements were made directly on these oxidized powders. Subsequently, all of the "POOL" sample powders from Expedition 352 have been analyzed onshore via wavelength-dispersive XRF methods (Godard et al 2015; Shervais et al 2016), permitting a more comprehensive evaluation of the different methods. Our shore based wavelength dispersive XRF measurements were made on

fused beads with 1:5 ratio of sample to Li-borate flux, and analyzed with a Panalytical 2400 XRF. Figure 4 presents pXRF:ICP-OES:XRF comparison plots for key elements in our "POOL" sample suite.

In Figure 4, it is evident that for all of these elements, there are systematic correlations within error between our pXRF results and results obtained on the ship via ICP-OES, and onshore via wavelength dispersive XRF. The correlations for each element vary in terms of slope and intercept, with some elements (Ti, K) showing intercepts very near zero, and slopes approaching 1.0. The Ca correlations versus the ICP-OES and XRF show slopes near 1.0, but the pXRF data are shifted to lower values, resulting in a non-zero intercept. These correlations are consistent with what was observed in the pXRF Ca correlation curve for standards in Figure 2. The pXRF Ti data shows scatter not evident in the other methods, which most likely relates to direct measurement of oxidized powders with pXRF, whereas the other two methods measured fusion beads, either in solution or in situ. We speculate that titanomagnetite grains were inhomogeneously distributed in some of the powders analyzed by pXRF.

For lower abundance elements, there are greater divergences in slopes among the pXRF:ICP-OES and pXRF:XRF correlations (Figure 4). Sr shows excellent agreement between the pXRF and XRF data with a slope near 1.0 and a near-zero intercept, while the shipboard ICP-OES results show greater scatter, albeit with considerable overlap. For Cr the pXRF:XRF and ICP-OES:XRF correlations are distinct, with the ICP-OES results showing lower Cr contents than pXRF below 300 ppm Cr, but higher concentrations than pXRF above this range, while the onshore XRF results were consistently higher. For Zr, the two correlations are overlapping, with the pXRF providing consistently lower values than either the ICP-OES or wavelength dispersive XRF, though given the relatively low concentrations in most of our samples the actual variation is rather modest.

The differences in determined concentrations between the pXRF, ICP-OES, and shore-based XRF systems are likely a function of calibration strategies and standard selection. In the case of the Niton pXRF, we imposed an external shipboard calibration based on a range of international reference samples on an existing factory-recommended Compton normalization calibration scheme for the SOILS protocol, that used the CCRMP TILL-4 glacial sediment reference material (Thermo Fisher 2010; CCRMP, 1995; Jochum et al 2005). Compton normalization schemes only work over limited ranges in concentrations, and are best for elements heavier than Ni, which may explain the problematic standards correlations for Fe

and Ca in Figure 2, as both run to higher values in our reference samples and recovered rocks than the TILL-4 standard. Our decision to generate correlation curves using a mixture of reference material types (basalts andesites, gabbros, boninites, and ultramafic rocks), while necessary to cover the concentration ranges in our recovered samples, may also have contributed to the variation in slope and intercept we observe in our Figure 4 correlations, as strongly different sample matrices can cause non-linear signal response on all of these instruments. With the shipboard ICP-OES, to minimize this problem we chose subsets of the reference samples in Table 2 for calibrating different sample runs, based on the unknowns we were analyzing (e.g., basaltic and gabbroic references samples for forearc basalts; boninite, andesite and ultramafic reference samples for boninites); but given our usage of the pXRF (see below) this kind of "tailoring" of our calibrations was not feasible.

Irrespective of the origins of the slope and intercept variations observed in Figure 4, the shipboard Niton pXRF produces data that *correlates systematically* with results from two well-established, but rather different quantitative elemental analysis methodologies. This demonstrates that:

a) The instrument can produce data for a selection of elements that, with suitable calibration, is both sufficiently precise and accurate, and
b) The data we collected under our described shipboard conditions can be easily corrected for direct comparisons to results by other methods.

Because the pXRF results correlate linearly with the results from other methods (ICP-OES, wavelength-dispersive XRF), these data can be used to construct a valid shipboard core chemostratigraphy in real time, while core recovery and/or logging are in progress. Furthermore, when widely separated core pieces are found to differ chemically, the pXRF makes it possible to rapidly analyze additional pieces in order to precisely define the location of chemostratigraphic boundaries.

3 Results and Discussion

The primary use of the pXRF during Expedition 352 was to conduct rapid geochemical measurements of volcanic rocks encountered in the recovered cores, both through direct measurements of cut rock surfaces on the archive-half core sections, and through the analysis of residual thin section billets for rock samples chosen for microscopic analysis. For these measurements, the sample holder system provided with the instrument was used to position smaller samples, and the shielded mounting system was used for longer core segments and

larger rock samples (Figure 1). A built-in digital video camera in the head of the instrument showed the 8 mm spot on the material that was to be analyzed, so positioning could be adjusted to avoid veins and/or clearly altered zones on rock surfaces.

Data for all calibrated elements were collected for all samples measured via pXRF. These data in some cases reproduced results for elements for which the ICP-OES afforded effective measurement (Ca, K_2O, TiO_2, Cr, Zr, Sr) and for some of these species (in particular TiO_2, K_2O and Sr) it offered an independent check on the accuracy of our shipboard ICP-OES results. Rubidium, zinc and copper, though included in the shipboard ICP-OES analytical protocols, were generally too low in concentration for successful measurement, so our pXRF data for these elements effectively augmented our shipboard elemental analysis capabilities. The comparable precision and accuracy of the pXRF data for powders and rock surface samples, and the consistency of its results with respect to other methods, meant that the extensive Expedition 352 pXRF rock surface database, collected for the purposes of chemostratigraphic correlation in our cores (see below), can be integrated with our shipboard ICP-OES results to provide a comprehensive geochemical profile of our recovered samples.

Ultimately, we used only a limited number of the elements measured via pXRF for routine unit definition and stratigraphic correlation within Expedition 352 drill cores, as necessitated by the constraints on time and resources aboard ship. As such, ours was a similar but more targeted approach to the collection and quantitative use of pXRF data than that described in Rowe et al (2012) and in other land-based studies. As key major elements (specifically, Mg and Si) were not analytically accessible via the pXRF at sea, we took the approach of using elemental proxies (e.g., Hastie et al 2007): abundances of the compatible element Cr were used to proxy MgO abundances; Ti abundances and Ti/Zr ratios were used to proxy SiO_2 as well as overall sample chemical depletion, and V abundances and V/Ti ratios were used to assay source and melt oxidation state, as a possible indicator of degree of prior melting of mantle sources for magmas (see Reagan et al, 2015). Strontium abundances were found to be comparatively unaffected by secondary alteration processes, and were thus useful in identifying the effects of plagioclase crystallization, and distinguishing between the weakly subduction affected fore-arc basalts and the strongly subduction modified boninites. Data for CaO and K_2O, both of which can be modified by secondary fluid-rock alteration processes, were useful in assaying the freshness of samples that were prepared for ICP-OES measurement on the ship, and in rectifying problems with shipboard ICP-OES measurements of recovered sediments, where the inability to completely decarbonate samples during Loss

on Ignition procedures led to problematic major element abundance totals. Ultimately, over 2000 individual pXRF analyses were made on rock surfaces and sample powders during Expedition 352.

Using the elemental proxies approach, the shipboard Petrology team developed a detailed chemostratigraphy for the recovered basalts from Sites U1440B and U1441A, and for the boninitic rocks recovered at Sites U1439C and U1442A (Reagan et al, 2015; Figures 5 and 6). In particular for the forearc basalts recovered from Hole U1440B, this chemostratigraphic record was essential to determining unit boundaries and constraining the volcanic stratigraphy of the core, as low recovery (~12%) during drilling and the highly uniform, aphyric nature of the recovered basalts provided few other means for resolving among eruptive units or tracking downhole changes (Figure 5).

In the boninite Holes U1439C and U1442A, relationships between the downhole chemostratigraphy and physical properties – specifically, magnetic susceptibility – became important in defining units, and in correlating what were ostensibly very different-looking downhole stratigraphies for two relatively closely located sites (<1 km apart; Figure 6). In both U1439C and U1442A, the detailed downhole geochemical record compiled via pXRF documented clear, progressive up-section declines in TiO_2 abundances, and increases in Cr abundances, pointing to a progressive depletion of the boninitic source mantle over time. These progressive changes in trace element abundances are associated with a transition from generally lower SiO_2 and more variably evolved boninite compositions toward the bottom of each section to higher SiO_2, more magnesian boninite compositions at the top of each section. These transitions are perhaps consistent with the early presence of some kind of persistent magma chamber in which differentiation of boninite parental magmas could occur, followed by eruptions of the more depleted, magnesian, and ostensibly primitive boninite lavas observed at the tops of both sequences.

The real-time, high-density geochemical results provided by the pXRF informed shipboard decisions on core segments to be prepared for shipboard ICP-OES analysis, and on the selection of the ~100 “POOL” samples that would be the focus of coordinated shore-based investigations. In addition, the pXRF data allowed the shipboard scientists to define boundaries between chemostratigraphic units precisely between adjacent core pieces, and guided selection of subsequent personal samples that will be used post-cruise to augment the POOL sample data.

The advantages of our pXRF capabilities were particularly evident toward the end of Expedition, when the ICP-OES ceased to be a viable analytical option due to its long lead-time for completing measurements, as well as during periods of high heave and/or transits, when ship movement precluded ICP operation. Our extensive pXRF dataset facilitated a more intensive and sophisticated at-sea analysis and interpretation of our recovered samples (e.g., Reagan et al 2015) than would have otherwise been possible. These data also proved crucial in the cost-benefit analyses of whether to continue or terminate drilling at a particular hole when difficulties were encountered.

The flexibility of the pXRF instrumentation and approach also permitted the quantitative re-examination of archived drill cores. During Exp. 352, we re-analyzed and directly compared the pXRF compositions of rock surfaces from the archive halves of cores from Deep Sea Drilling Program (DSDP) Leg 60 (Mariana forearc) to those of samples from our Expedition, confirming their geochemical kinship and clarifying the chemical differences between samples from these two different localities. Limitations on pXRF capabilities associated with cores containing significant pore water, as had been reported on in past efforts with shipboard X-ray core scanning instruments (i.e., Kido et al 2006; Weltje and Tjallingi 2008; Hennekem and de Lange 2012) were not an issue with the samples recovered on Expedition 352. The fine-grained and uniform nature of many of our recovered samples made Expedition 352 a nearly ideal testbed for this analytical tool and approach, though the robust and flexible nature of the instrumentation suggests that even with less ideal sample types (i.e., coaser grained gabbroic/granitic rocks) useful results could be obtained with proper precautions.

4 Conclusions

Modern energy-dispersive portable XRF analyzers permit the reproducible quantitative determination of a menu of major and trace elements from Z=19 to Z=40 without atmosphere control or other concerns typically encountered with XRF systems. We developed data correction protocols for the portable X-ray fluorescence spectrometer on the *JOIDES Resolution,* and used the instrument to make rapid and precise quantitative abundance measurements on a menu of key elements. The robustness of the pXRF in analyzing rock surfaces and powders permitted us to obtain rapid, high density results on freshly recovered core materials, which made the instrument a highly valued addition to our shipboard analytical capabilities during IODP Expedition 352. With an awareness of the limitations and

constraints of the method, and care in the instrument's calibration, portable X-ray fluorescence spectrometers can provide important new capabilities for rapid, quantitative sample characterization at sea, and offer critical information to operational decision making onboard geoscience research vessels.

Acknowledgements

The lead author would like to thank Dr. Yigang Xu and co-author Hong Yan Li of the Guangzhou Institute of Geochemistry, Chinese Academy of Sciences for hosting him for an extended research visit in early 2016, during which time this manuscript was finally completed. Thanks also to the JRSO technical staff on the JOIDES Resolution during Expedition 352 for walking the lead author by the hand through the specifics of the Thermo-Fisher Niton pXRF use, and for their ongoing support and patience with us as the experiment went industrial; as well as to the JRSO staff in College Station, TX for ensuring that their pXRF got back on the *JR* for our expedition after repairs. We thank Editor Catherine Chauvel, Jorg Geldmacher and an anonymous reviewer for comments and feedback that substantially improved this paper. This work was supported by the International Ocean Discovery Program, and the science support programs of all the participating nations represented on Expedition 352; as well as NSF grants OCE1558855 to J. Ryan, OCE1558689 to J. Shervais, OCE1558647 to M. Reagan, and Chinese Science Foundation grant GASI-GEOGE-02 to H-Y. Li.

.

References

Canadian Certified Reference Materials Project, 1995, Certificate of Analysis, Provisional Values, Till-1, Till-2, Till-3, and Till-4, Geochemical Soil and Till Reference Materials.

Christie DM, Pedersen RB, Miller DJ, Shipboard Scientific Party, 2001, Mantle reservoirs and migration associated with Australian-Antarctic rifting. Proceedings of the ODP, initial reports 187. http://www-odp.tamu.edu/publications/187_IR/ 187ir.htm

Conrey, R.M., Goodman-Elgar, M., Bettencourt, N., Seyfarth, A., Van Hoose, A., and Wolff, J.A., 2014, Calibration of a portable X-ray fluorescence spectrometer in the analysis of archaeological samples using influence coefficients. *Geochemistry: Exploration, Environment, Analysis*, Geol. Soc. London, http://dx.doi.org/10.1144/geochem2013-198

Drake, L., 2014, XRF User guide: Concepts, http://www.xrf.guru/styled-12/page67/index.html

Gillis, K.M., Snow, J.E., Klaus, A., and the Expedition 345 Scientists, 2014, *Proceedings of the Integrated Ocean Drilling Program, 345*: College Station, TX (International Ocean Discovery Program). http://dx.doi.org/10.2204/iodp.proc.345.2014

Godard, M., Ryan, J.G., Shervais, J., Whattam, S., Sakuyama, T., Kirchenbaur, M., Li, H., Nelson, W., Prytulak, J., Pearce, J., Reagan, M, and the Expedition 352 Scientific Team, 2015, Geochemistry of Bonin fore-arc volcanic sequence: results from IODP Expedition 352. 2015 AGU Fall Meeting, Abstract T41E-2948.

Hastie, A.R., Kerr, A.C., Pearce, J.A., and Mitchell, S.F., 2007, Classification of altered Volcanic island arc rocks using immobile trace elements: development of the Th–Co discrimination diagram, Jour. Petrol., 48, 2341-2357, 2007.

Hennekam, R., and de Lange, G., 2012, X-ray fluorescence core scanning of wet marine sediments: methods to improve quality and reproducibility of high resolution paleoenvironmental records, Limnol. Oceanogr.: Methods, 10, 991–1003

Hu, W., Huang, B., Weindorf, D.C., and Chen, Y., 2014, Metals analysis of agricultural soils via portable X-ray fluorescence spectrometry. Bull. Environ. Contam. Toxicol., 92, 420–426.

Jan Weltje, G., and Tjallangii, R., 2008, Calibration of XRF core scanners for quantitative geochemical logging of sediment cores: Theory and application. Earth Planet. Sci. Lett., 224, 423-438.

Jochum, K.P., Nohl, U., Herwig, K., Lammel, E., Stoll, B., Hofmann A.W., 2005, GeoReM: A new geochemical database for reference materials and isotopic standards. Geostandards and Geoanalytical Research, 29, 333-338.

Kido, Y., Koshikawa, T., and Tada, R., 2006, Rapid and quantitative major element analysis method for wet, fine-grained sediments using an XRF microscanner, Marine Geology, 229, 209–225

Koppers, A.A.P., Yamazaki, T., Geldmacher, J., and the Expedition 330 Scientists, 2012. *Proceedings of the Integrated Ocean Drilling Program, 330*: Tokyo (Integrated Ocean Drilling Program Management International, Inc.).
http://dx.doi.org/10.2204/iodp.proc.330.2012

Liang, L., Sun, Y., Yao, Z., Liu, Y., and Wu, F., 2012, Evaluation of high-resolution elemental analyses of Chinese loess deposits measured by X-ray fluorescence core scanner, Catena, 92, 75-82.

Lowemark, L., Chen, H.-F., Yang, T.-N., Kylander, M., Y.-W. Hsu, T.-Q. Lee, Song, S.-R., and Jarvis, S., 2011, Normalizing XRF-scanner data: A cautionary note on the interpretation of high-resolution records from organic-rich lakes, Journal of Asian Earth Sciences, 40, 1250-1256.

Potts, P.J., 1992, *A Handbook of Silicate Rock Analysis*. New York, Springer Science Business Media, 630 p.

Potts, P.J., and West, M. (eds.), 2008, *Portable X-ray Fluorescence Spectrometry: Capabilities for In Situ Analysis.* Royal Society of Chemistry, http://pubs.rsc.org | doi:10.1039/9781847558640-00001

Reagan, M.K., Ishizuka, O., Stern, R.J., Kelley, K.A., Ohara, Y., Blichert-Toft, J., Bloomer, S.H.., Cash, J., Fryer, P., Hanan, B.B., Hickey-Vargas, R., Ishii, T., Kimura, J-I., Peate, D.W., Rowe, M.C., and Woods, M., 2010, Fore-arc basalts and subduction initiation in the Izu-Bonin-Mariana system. Geochemistry Geophysics Geosystems, 11, Q03X12, doi:10.1029/2009GC002871

Reagan, M.K., Pearce, J.A., Petronotis, K.E., and the Expedition 352 Scientists, 2015, *Proceedings of the International Ocean Discovery Program: Volume 352: Izu-Bonin-Mariana Fore Arc*. doi:/10.14379/iodp.proc.352.2015.

Reynolds, R.C. Jr., 1963, Matrix corrections in trace element analysis by X-ray fluorescence: estimation of mass absorption coefficient by Compton scattering. American Mineralogist, 48, 1133-1143.

Rowe, H., Hughes N., and Robinson, K., The quantification and application of handheld energy-dispersive x-ray fluorescence (ED-XRF) in mudrock chemostratigraphy and geochemistry, Chem. Geol., 324-325, 122-131.

Shervais, J., Haugen, E., Ryan, J.G., Godard, M., Prytulak, J., Shimizu, K., Chapman, T., Nelson, W., Heaton, D., Li, H., Kirchenbaur, M., Li, Y., Whattam, S., Reagan, M., and Pearce, J. (2016) Chemostratigraphy of subduction initiation: IODP Expedition 352 boninite and FAB. Geological Society of America Abstracts with Programs, 48:7, doi: 10.1130/abs/2016AM-283837

Swanhart, S., Weindorf, D.C., Chakraborty, S., Bakr, N., Zhu, Y., Nelson, C., Shook, K., and Acree, A., 2014, Soil salinity measurement via portable X-ray fluorescence spectrometry. Soil Sci., 179, 417–423.

Teagle, D.A.H., Ildefonse, B., Blum, P., and the Expedition 335 Scientists, 2012, *Proceedings of the Integrated Ocean Drilling Program, 335*, Tokyo (Integrated Ocean Drilling Program Management International, Inc.), http://dx.doi.org/10.2204/iodp.proc.335.2012

Thermo Scientific, 2010, *Thermo Fisher Scientific Niton Analyzers: XL3 Users Guide, Version 7.0, Revision A.*

Thermo Scientific, 2016, Thermo Scientific Niton XL3t GOLDD+ Portable XRF Analyzer. [http://pdf.directindustry.com/pdf/thermo-fisher-scientific/thermo-scientific-niton-xl3t-goldd-spec-sheet/25842-152207.html]

Tykot, R.H., Using nondestructive portable X-ray fluorescence spectrometers on stone, ceramics, metals, and other materials in museums: advantages and limitations, Appl. Spectroscopy, 70, 42-56, 2016.

US Environmental Protection Agency, 2007, Method 6200. Field portable X-ray fluorescence spectrometry for the determination of elemental concentrations in soil and sediment. http://www.epa.gov/sites/production/files/2015-12/documents/6200.pdf .

Weindorf, D.C., Zhu, Y., McDaniel P., Valerio, M., Lynn, L., Michaelson, G., Clark M, and Ping, C.L., 2012, Characterizing soils via portable x-ray fluorescence spectrometer: 2. spodic and albic horizons. Geoderma, 189-190, 268-277.

Wien, K., Wissman, D., Kolling, M. and Schulz, H.D., 2005, Fast application of X-ray fluorescence spectrometry aboard ship: how good is the new portable Spectro Xepos analyser? Geo-Marine Letters, 25, 248-264.

Zhu, Y., Weindorf, D.C., and Zhang, W., 2011, Characterizing soils using a portable X-

ray fluorescence spectrometer: 1. Soil texture. Geoderma, 167-168, 167-177.

Figures:

Figure 1. Photographs of the shipboard Fisher-Niton GOLDDxlt pXRF instrument and its two different sample mounts, after Reagan et al (2015). a) The pXRF mounted in its "Field Mate" sample holder. b) The IODP-made holder for longer core samples. The pXRF mounts from below. Samples are placed on rectangular aperture visible in the shielded sample chamber.

Figure 2: Working curves constructed for the elements analysed by pXRF, essentially plots of pXRF measured concentrations vs. accepted values for the reference materials examined. Standard reference materials used included BHVO-2, BCR-2, JB-2, JB-3, AGV-1, MRG-1, JP-1, and DTS-1; consensus values from GeoREM (Jochum et al 2005). Also included were boninite samples CHI 40618, CHI 32108, and CHI 88X (Pearce, unpublished data), to extend our concentration ranges into those likely to be encountered in Expedition 352 boninite samples. a) K_2O. b) TiO_2. c) CaO. d) Sr. e) Rb. f) Cr. g) Fe_2O_3. h) Zn. i) V. j) MnO. k)Cu.

Figure 3: Plots of a)TiO_2, b)CaO, c)K_2O, d)Sr, e)Cr, and f)Zr for U1440B sample powders and associated thin section residues. Uncertainties are as reported by the pXRF. Solid lines and the associated equations are linear regression correlations for the data, and dotted lines reflect 95% confidence intervals. The elements least affected by secondary alteration processes show the most uniformity between powdered and solid samples.

Figure 4: Plots of a) a)TiO_2, b)CaO, c)K2O, d)Cr, e)Sr, and f)Zr for Hole U1440B samples comparing pXRF (red circles), and wavelength dispersive XRF (blue triangles) to shipboard ICP-OES results on Expedition 352 "POOL" sample powders. Wavelength dispersive XRF results are from Shervais et al (2016) and Godard et al (2015). Regression lines, equations, and 95% confidence intervals as in Figure 3.

Figure 5: Chemostratigraphic correlation plots after Reagan et al (2015) from IODP Expedition 352 Site U1440B, highlighting the use of TiO_2 and Cr concentrations to identify different magmatic units, despite very poor sample recovery (~12%).

Figure 6: Correlations between Ti/Zr, Cr, and magnetic susceptibility for IODP Expedition 352 Holes U1439C and U1442A, from Reagan et al (2015), along with a comparative outline

of the occurrences of high-silica and low-silica boninites in each section, as well as positions of observed zones of melt mixing. The linked geochemical and physical property relationships were used both to define magmatic units downhole, and to document the marked stratigraphic differences between the two nearby (<1 km apart) sites.

Tables:

Table 1: List of elements measured via pXRF during IODP Expedition 352, analytical conditions and detection limits.

Table 2: Standard Reference Materials used in pXRF onshore calibration and to construct pXRF data correction curves. Standard data based on consensus values from GeoReM (Jochum et al 2005); boninite data from J. Pearce.

Table 3: Long-term reproducibility of the shipboard Fisher Niton GOLDD+XL3t portable XRF instrument.

Table 4: pXRF reproducibility and accuracy on rock surfaces.

Fig 1

a.

b.

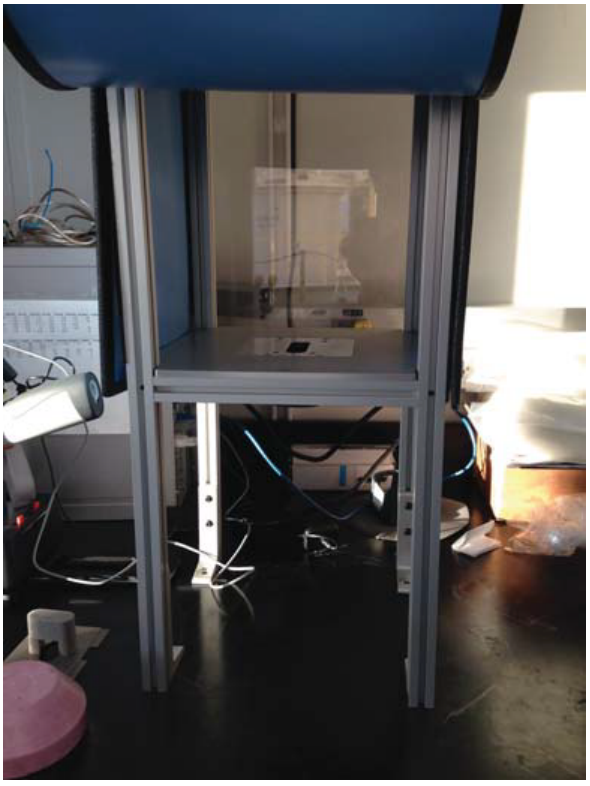

Fig 2 a, b, c

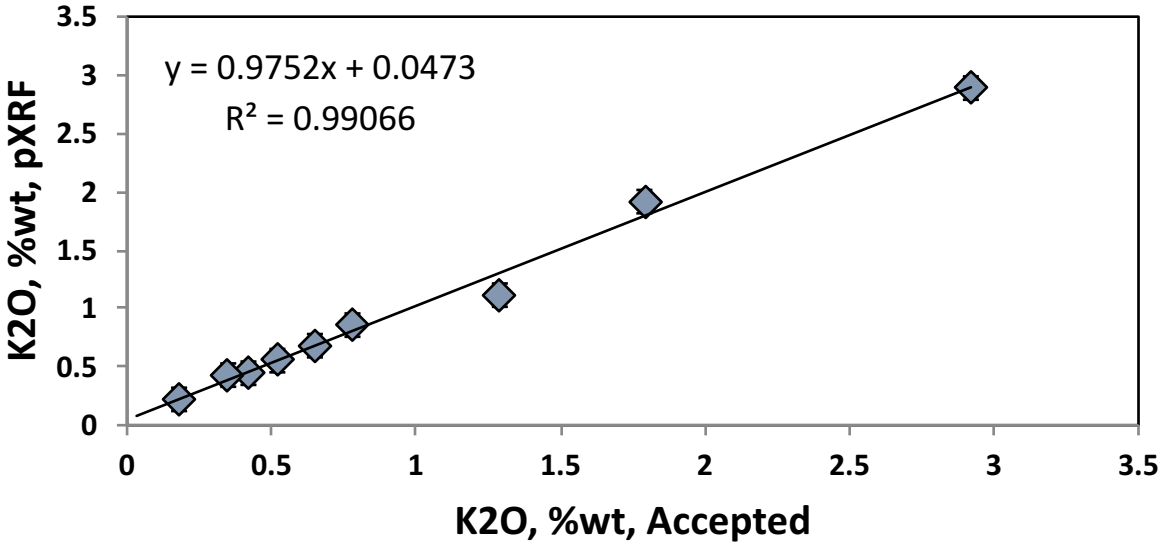
y = 0.9752x + 0.0473
R² = 0.99066
K2O, %wt, pXRF
K2O, %wt, Accepted
0
0.5
1
1.5
2
2.5
3
3.5

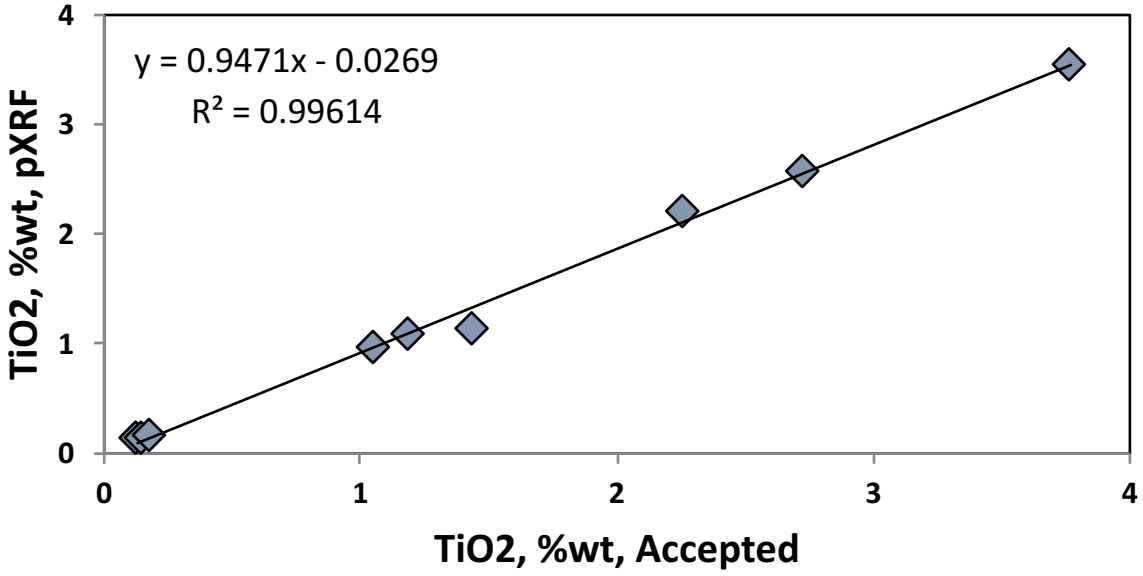
y = 0.9471x - 0.0269
R² = 0.99614
TiO2, %wt, pXRF
TiO2, %wt, Accepted
0
1
2
3
4

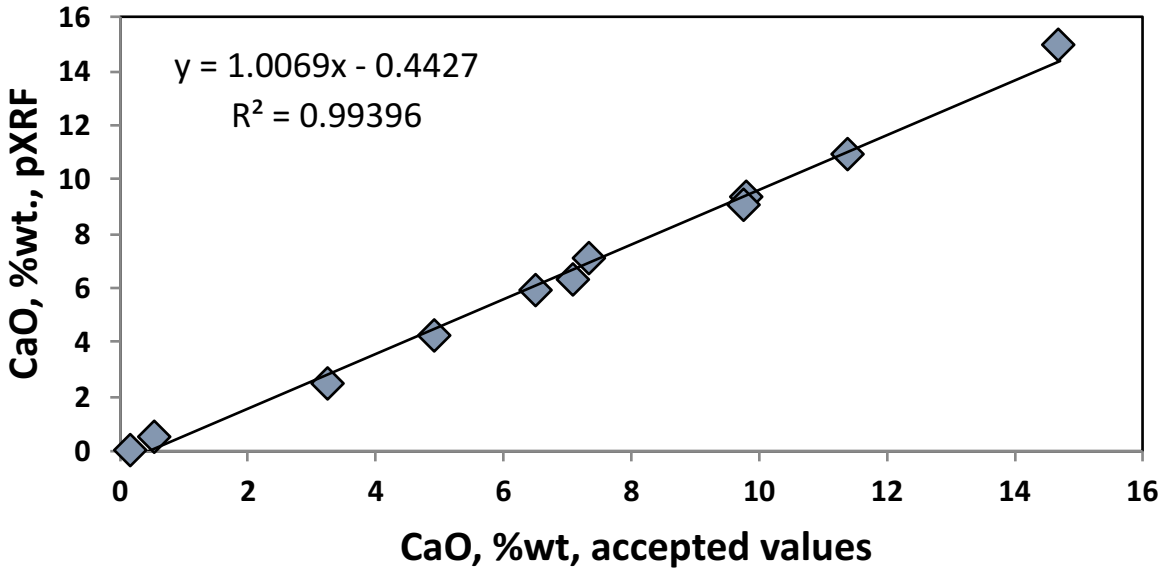
y = 1.0069x - 0.4427
R² = 0.99396
CaO, %wt., pXRF
CaO, %wt, accepted values
0
2
4
6
8
10
12
14
16

Fig 2 d,e,f

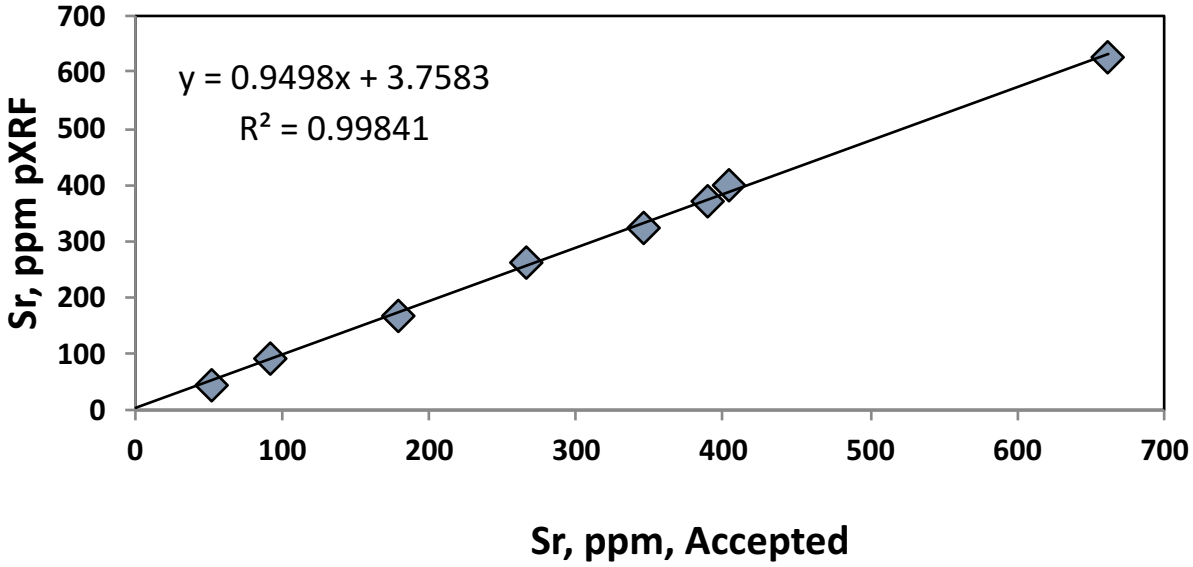
y = 0.9498x + 3.7583
R² = 0.99841
Sr, ppm pXRF
Sr, ppm, Accepted
0
100
200
300
400
500
600
700

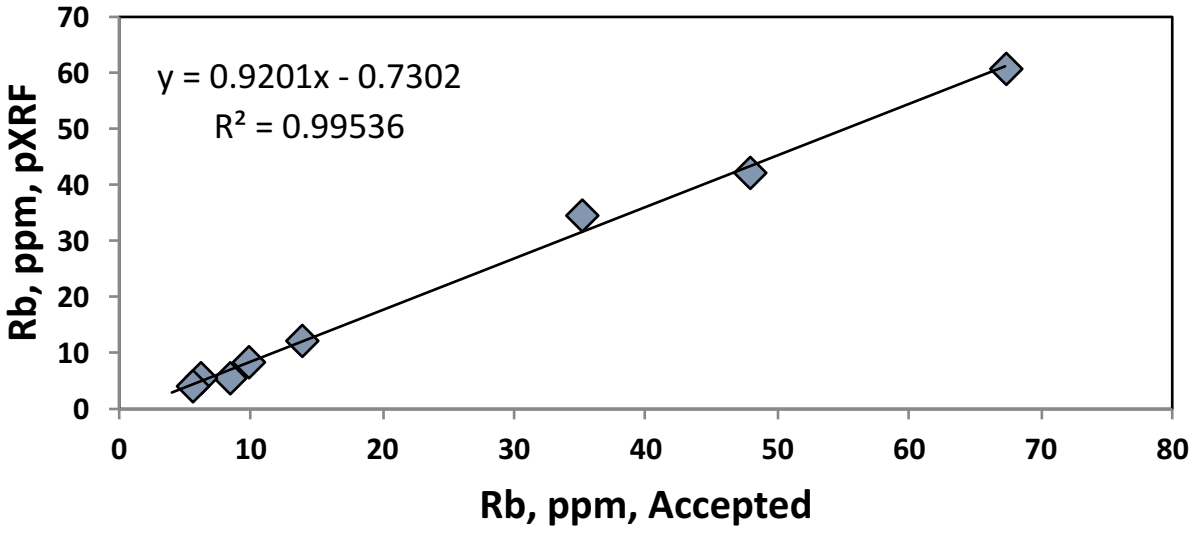
y = 0.9201x - 0.7302
R² = 0.99536
Rb, ppm, pXRF
Rb, ppm, Accepted
0
10
20
30
40
50
60
70
80

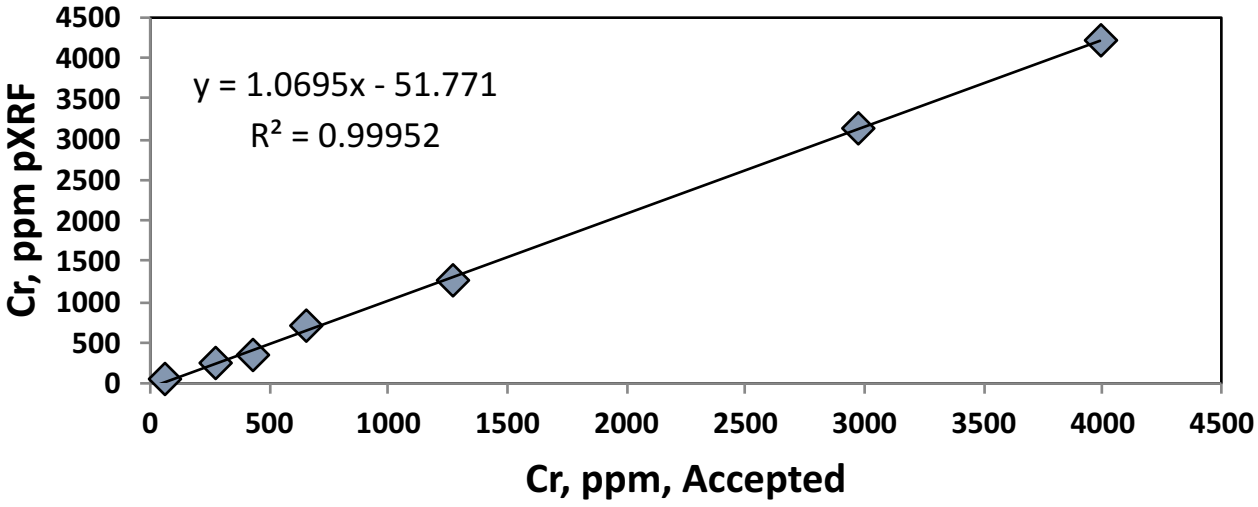
y = 1.0695x - 51.771
R² = 0.99952
Cr, ppm pXRF
Cr, ppm, Accepted
0
500
1000
1500
2000
2500
3000
3500
4000
4500

Fig 2 g,h,i

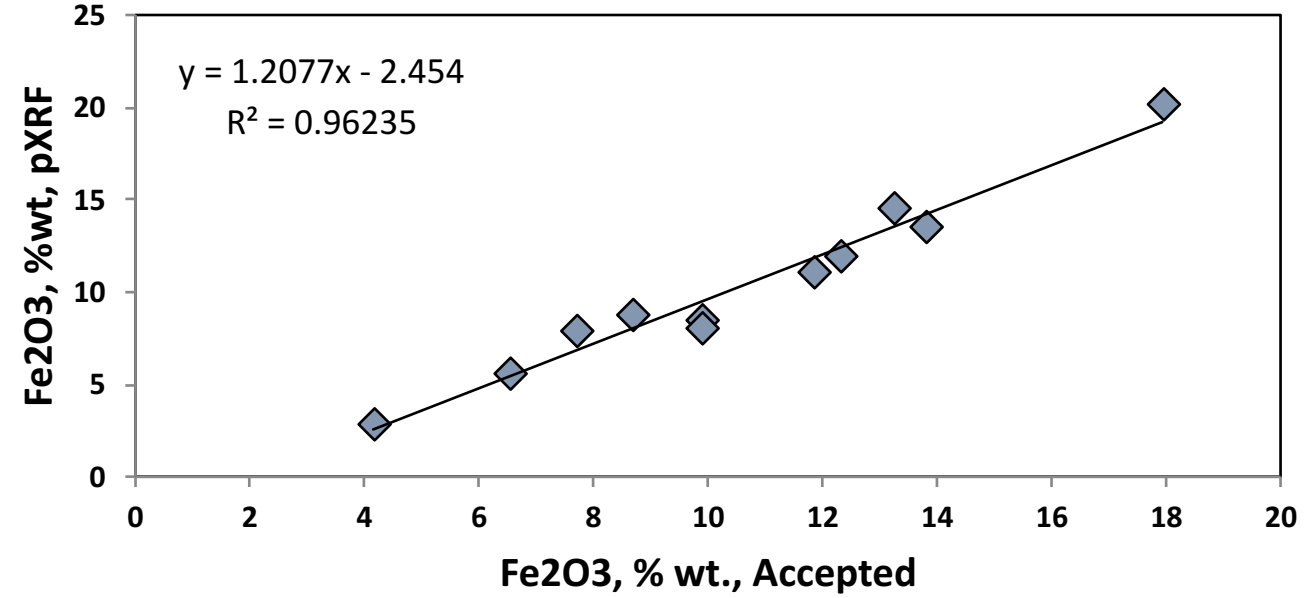
y = 1.2077x - 2.454
R² = 0.96235
Fe2O3, %wt, pXRF
Fe2O3, % wt., Accepted
0
5
10
15
20
25
0
2
4
6
8
10
12
14
16
18
20

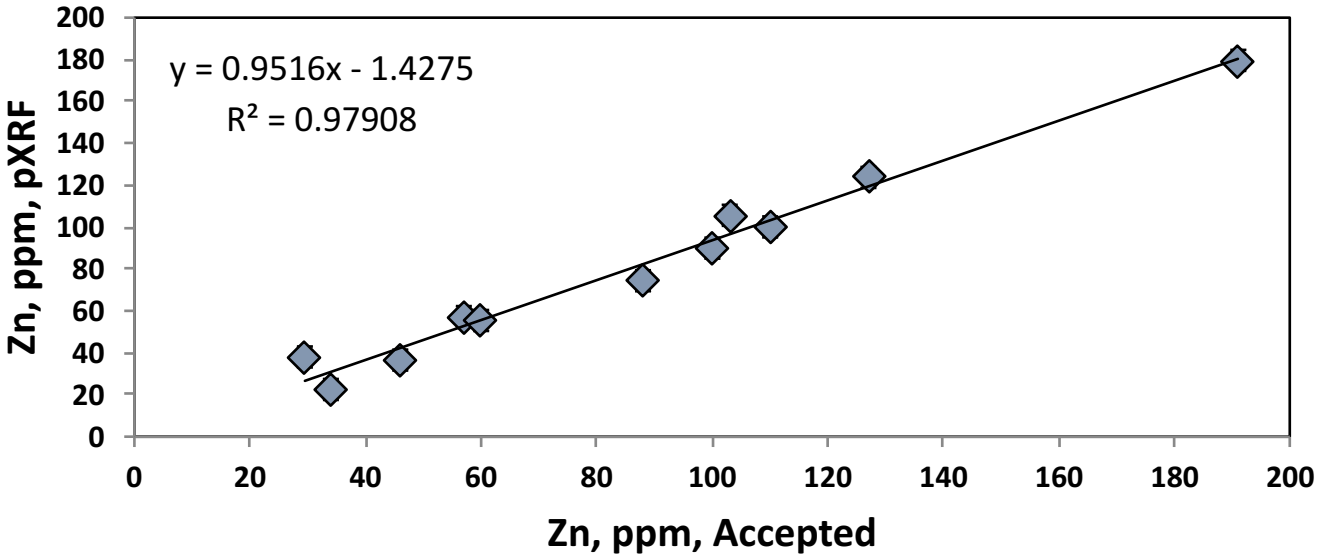
y = 0.9516x - 1.4275
R² = 0.97908
Zn, ppm, pXRF
Zn, ppm, Accepted
0
20
40
60
80
100
120
140
160
180
200

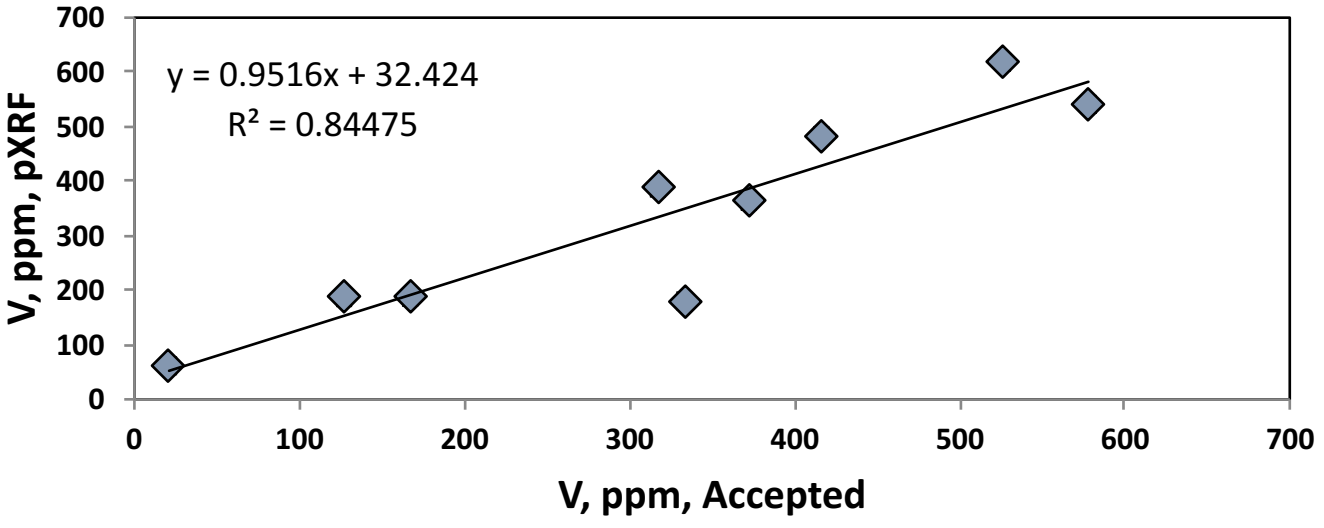
y = 0.9516x + 32.424
R² = 0.84475
V, ppm, pXRF
V, ppm, Accepted
0
100
200
300
400
500
600
700

Figure 2 j,k

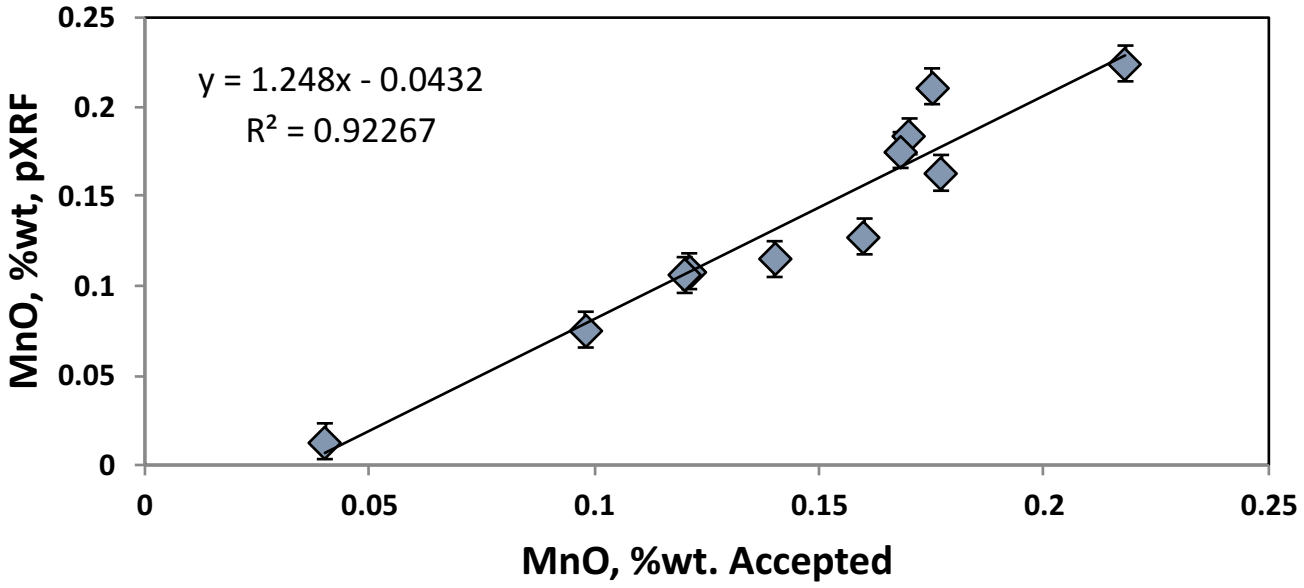
y = 1.248x - 0.0432
R² = 0.92267
MnO, %wt, pXRF
MnO, %wt. Accepted
0
0.05
0.1
0.15
0.2
0.25

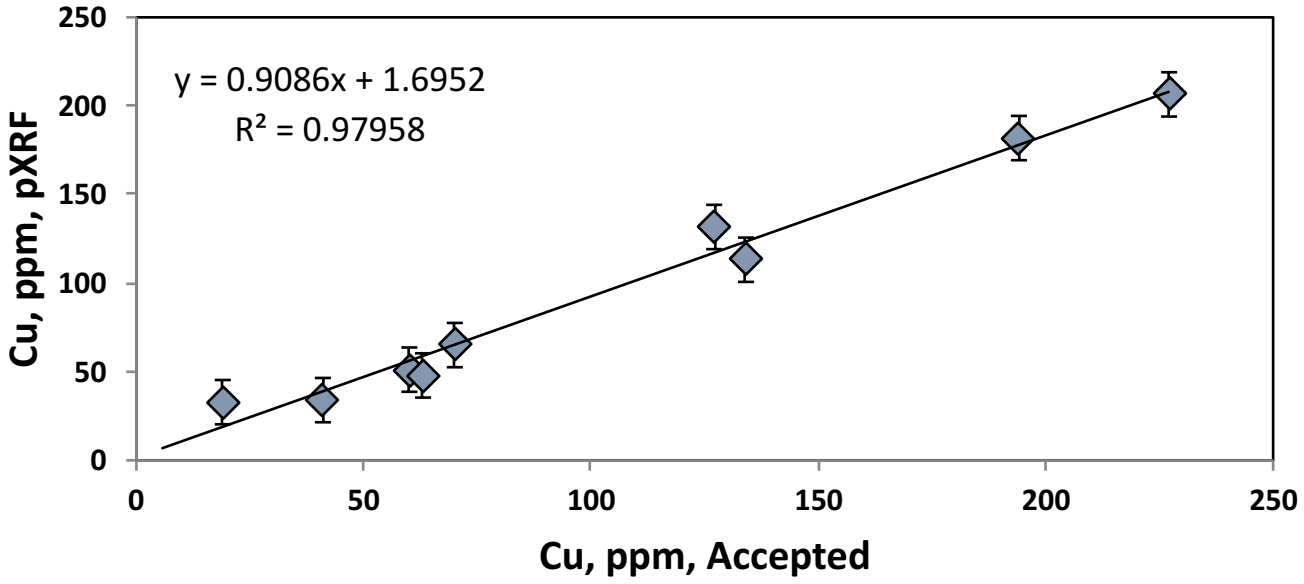
y = 0.9086x + 1.6952
R² = 0.97958
Cu, ppm, pXRF
Cu, ppm, Accepted
0
50
100
150
200
250

Figure 3

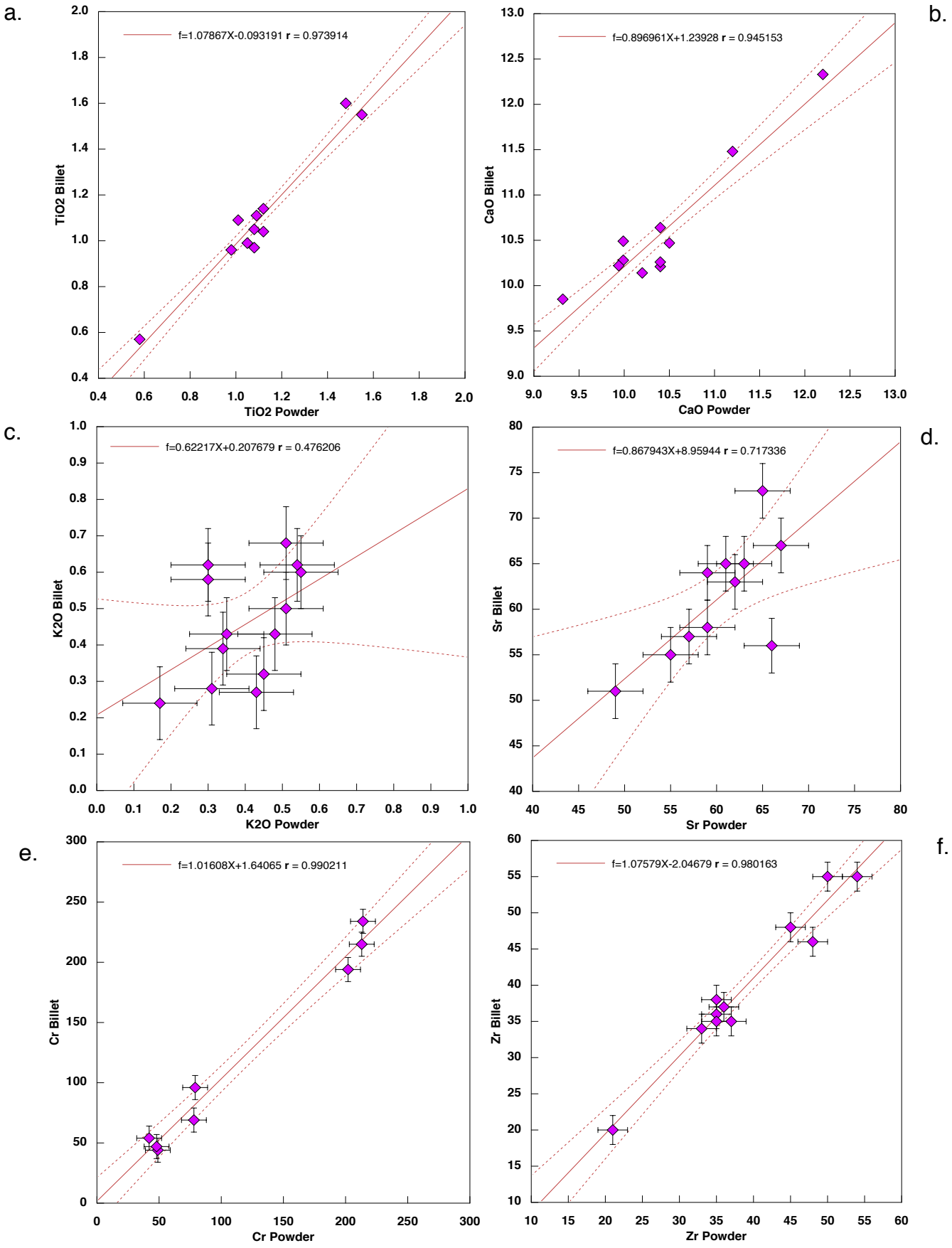
a.
f=1.07867X-0.093191 r = 0.973914
TiO2 Billet
TiO2 Powder
b.
f=0.896961X+1.23928 r = 0.945153
CaO Billet
CaO Powder
c.
f=0.62217X+0.207679 r = 0.476206
K2O Billet
K2O Powder
d.
f=0.867943X+8.95944 r = 0.717336
Sr Billet
Sr Powder
e.
f=1.01608X+1.64065 r = 0.990211
Cr Billet
Cr Powder
f.
f=1.07579X-2.04679 r = 0.980163
Zr Billet
Zr Powder

Figure 4

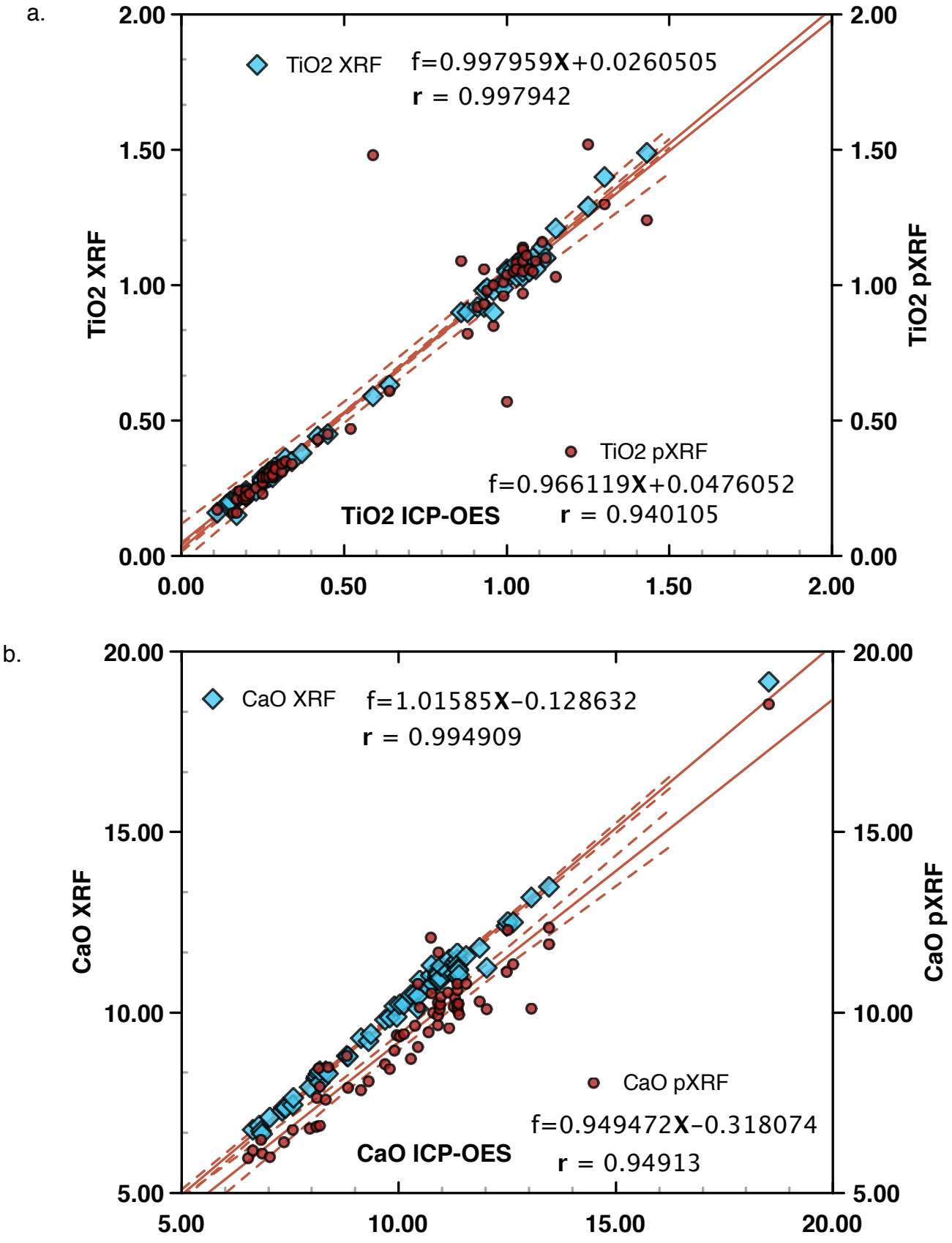
a.
TiO2 XRF
f=0.997959X+0.0260505
r = 0.997942
TiO2 pXRF
f=0.966119X+0.0476052
r = 0.940105
TiO2 ICP-OES
TiO2 XRF
TiO2 pXRF
0.00
0.50
1.00
1.50
2.00
b.
CaO XRF
f=1.01585X-0.128632
r = 0.994909
CaO pXRF
f=0.949472X-0.318074
r = 0.94913
CaO ICP-OES
CaO XRF
CaO pXRF
5.00
10.00
15.00
20.00

c.

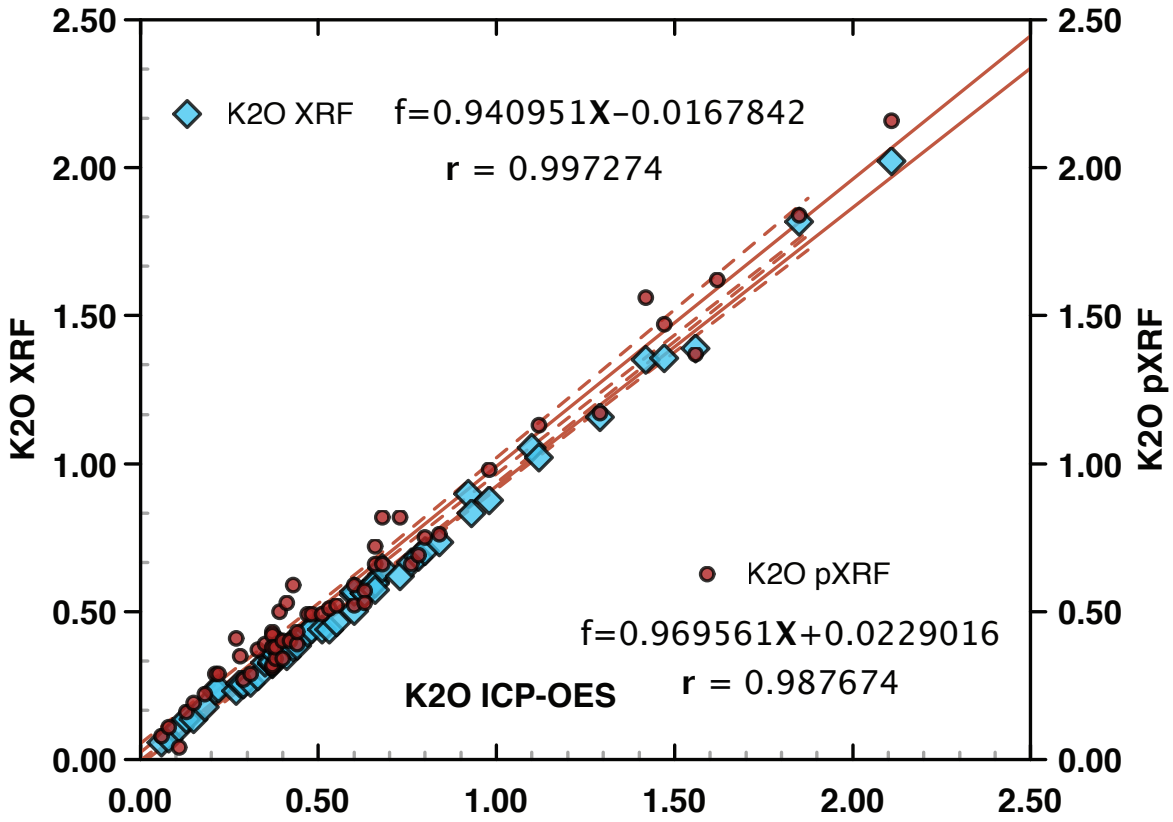
K2O XRF
f=0.940951X-0.0167842
r = 0.997274
K2O pXRF
f=0.969561X+0.0229016
r = 0.987674
K2O ICP-OES
K2O XRF
K2O pXRF
0.00
0.50
1.00
1.50
2.00
2.50

d.

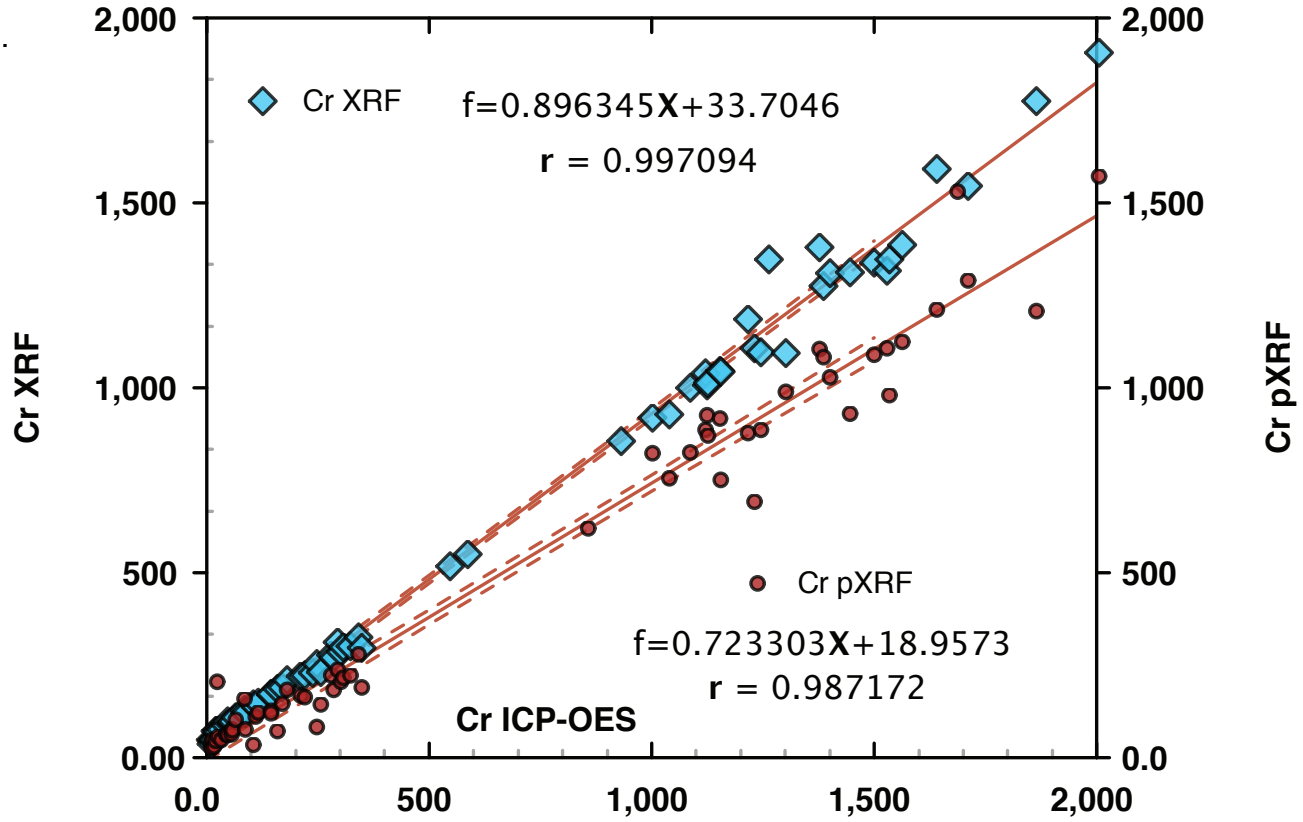
Cr XRF
f=0.896345X+33.7046
r = 0.997094
Cr pXRF
f=0.723303X+18.9573
r = 0.987172
Cr ICP-OES
Cr XRF
Cr pXRF
0.0
500
1,000
1,500
2,000

e.

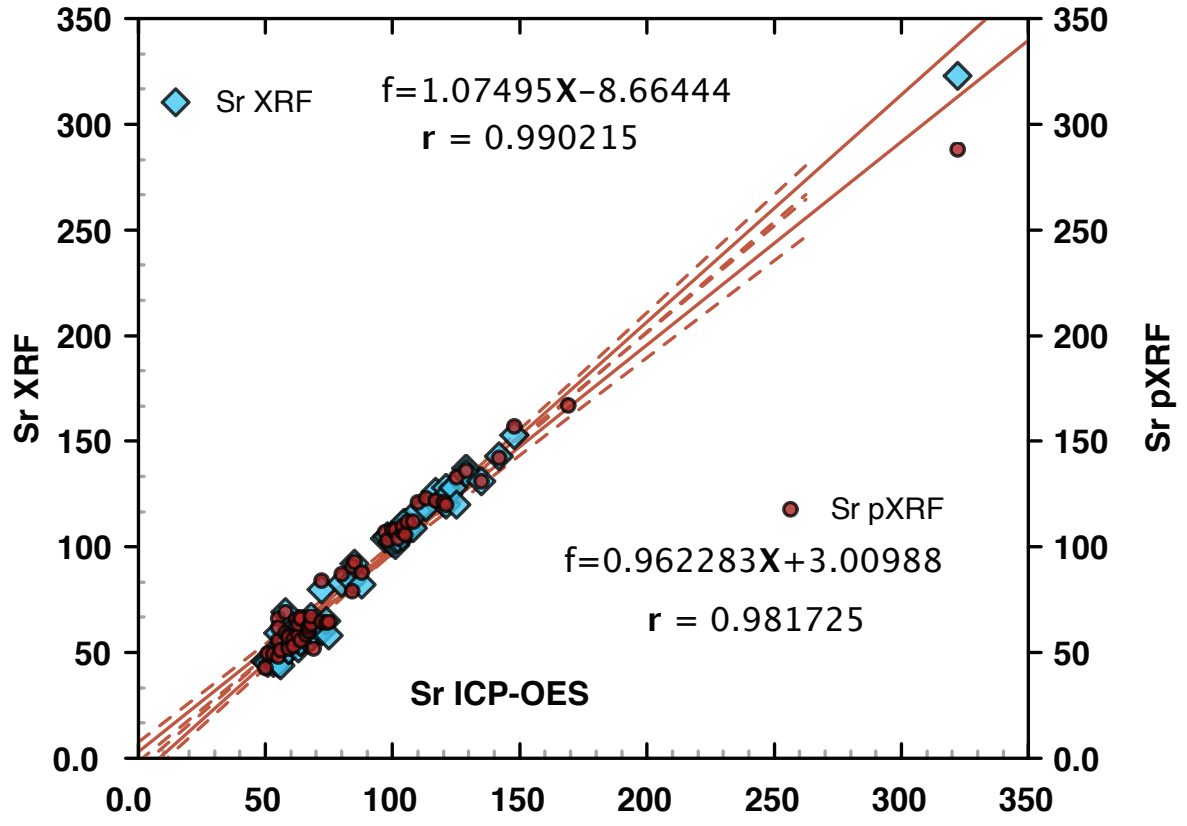
Sr XRF
f=1.07495X-8.66444
r = 0.990215
Sr pXRF
f=0.962283X+3.00988
r = 0.981725
Sr ICP-OES
Sr XRF
Sr pXRF
0.0
50
100
150
200
250
300
350

f.

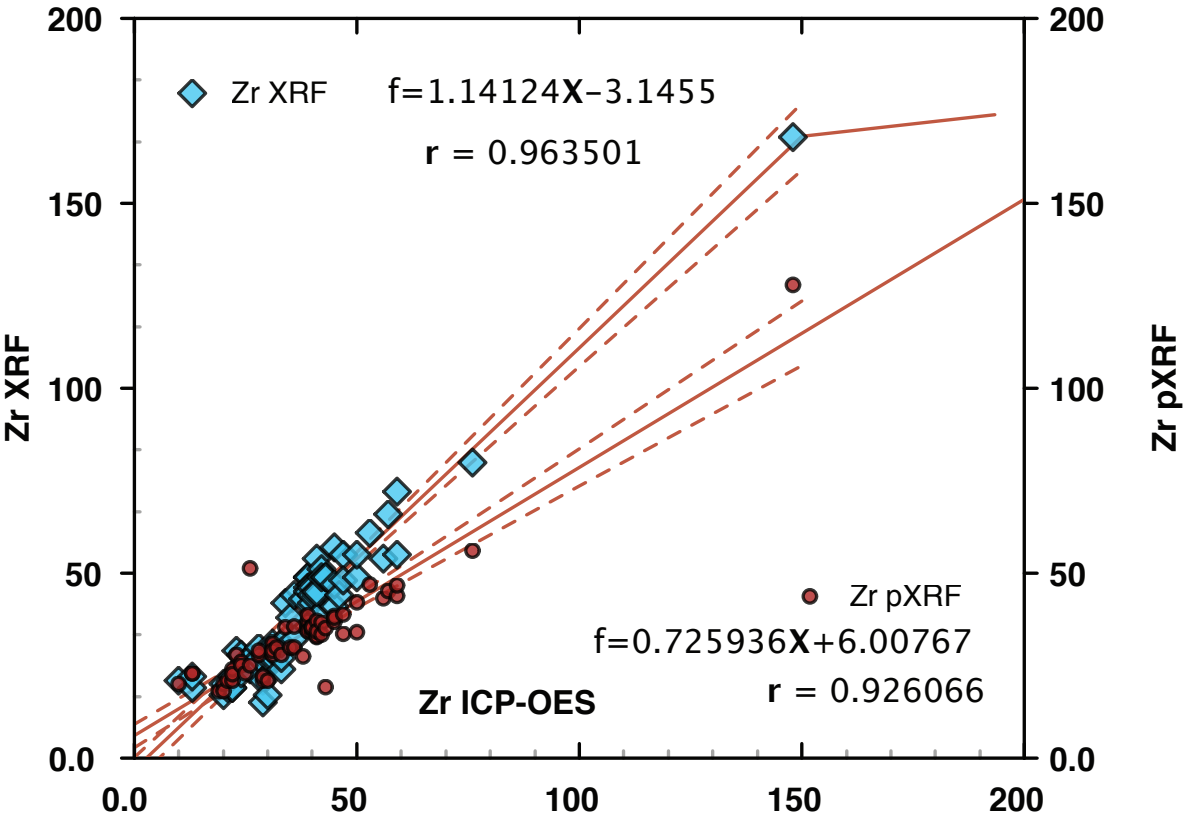
Zr XRF
f=1.14124X-3.1455
r = 0.963501
Zr pXRF
f=0.725936X+6.00767
r = 0.926066
Zr ICP-OES
Zr XRF
Zr pXRF
0.0
50
100
150
200

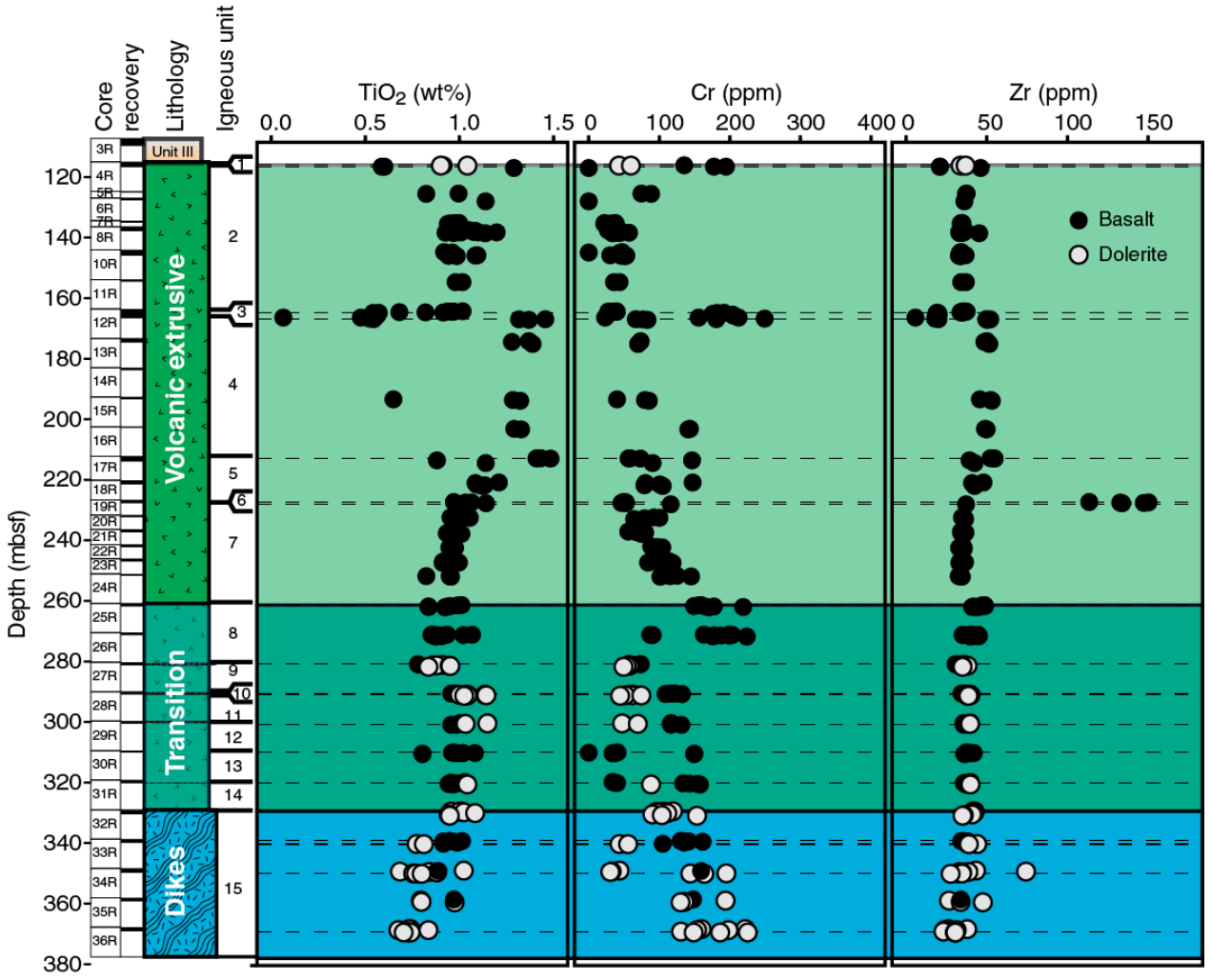
Core recovery
Lithology
Igneous unit
TiO2 (wt%)
Cr (ppm)
Zr (ppm)
Depth (mbsf)
Unit III
Volcanic extrusive
Transition
Dikes
Basalt
Dolerite

Figure 5

Figure 6

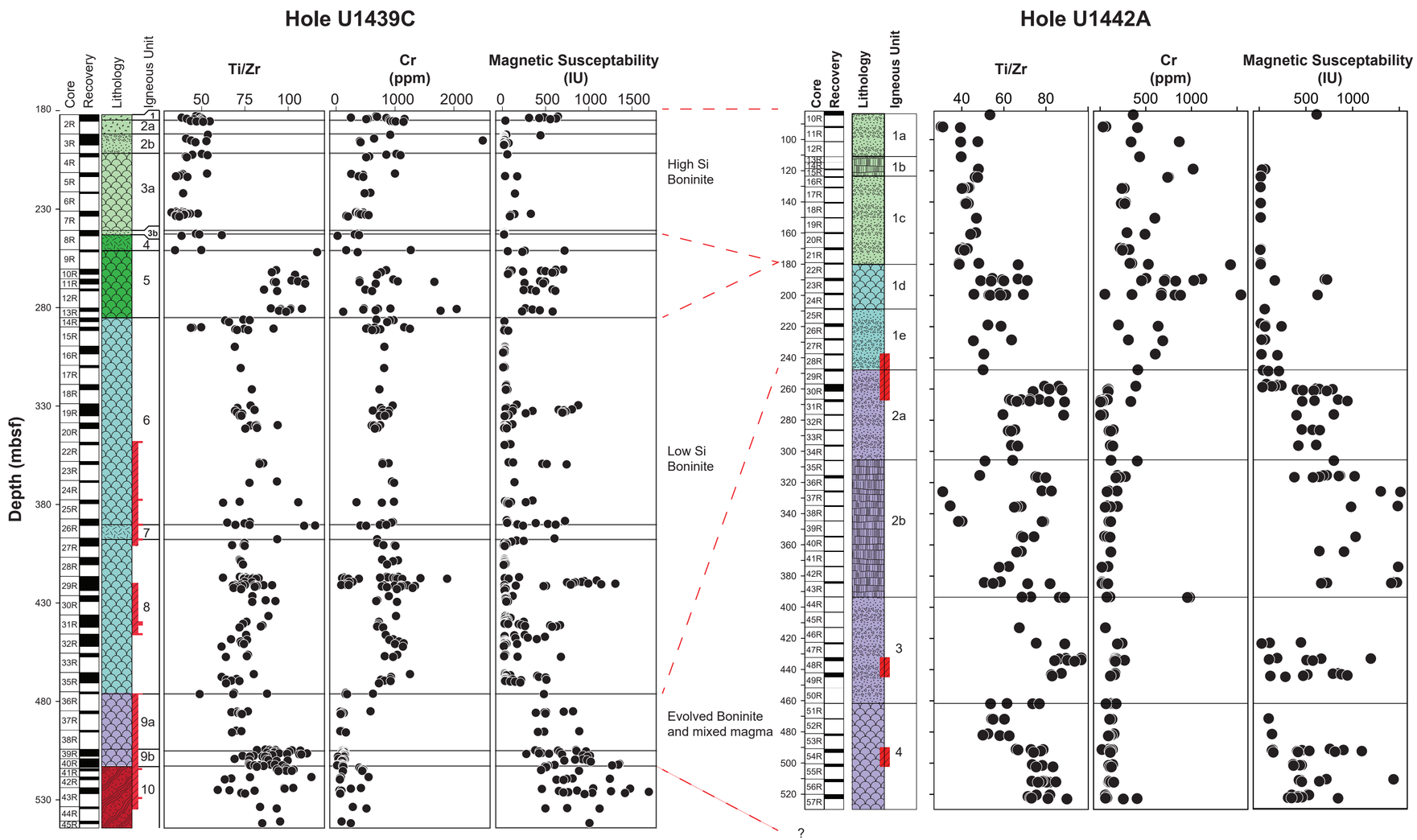
Hole U1439C
Hole U1442A
Depth (mbsf)
Core
Recovery
Lithology
Igneous Unit
Ti/Zr
Cr (ppm)
Magnetic Susceptability (IU)
High Si Boninite
Low Si Boninite
Evolved Boninite and mixed magma
?

Revised tables in pdf format

Click here to download Table: Revised pXRF paper tables.pdf

Table 1: Reference materials used in pXRF on-shore calibration, and to construct pXRF correction curves

	TiO2 (wt%)	Fe2O3 (wt%)	CaO (wt%)	K2O (wt%)	Zr (ppm)	Sr (ppm)	Rb (ppm)	Zn (ppm)	Cu (ppm)	MnO (wt%)	Cr (ppm)	V (ppm)
Shore-based calibration (Compton Normalization)												
CCRMP TILL-4	0.81	5.63	1.25	3.25	385	109	161	70	237	0.06	53	67
Shipboard calibration:												
BHVO-2	2.73	12.25	11.4	0.52	172	396	9.11	103	127	0.168	280	317
BCR-2	2.36	13.8	7.12	1.79	188	346	48	127	19	0.175	18	416
JB-2	1.19	13.22	9.82	0.42	52	178	6.2	110	227	0.218	27.4	578
JB-3	1.44	11.84	9.79	0.78	97.8	403	15.1	100	194	0.177	58.1	372
AGV-1	1.05	6.52	4.94	2.92	227	662	67.3	88	60	0.098	10.1	333
DTS-1	0.005	8.68	0.17	0.001	4	0.32	0.058	46	7.1	0.121	3990	11
MRG	3.77	17.93	14.71	0.18	108	266	8.5	191	134	0.17	430	526
JP-1	--	7.7	0.56	0.033	6	3.3	4	29.5	5.7	0.12	2970	29
CH40618*	0.13	9.9	6.53	0.35	13.2	51	5.7	57	41	0.14	1275	167
CH32108*	0.15	9.87	7.37	0.65	20.5	239	14	60	70	0.16	660	127
CHX88A*	0.18	4.15	3.28	1.29	54.5	91	35.2	34	63	0.04	10	21

USGS, GSJ and CCRMP reference materials data from Jochum et al (2005)

* Data from J. Pearce, unpublished

Table 2: List of elements measured via pXRF during IODP Expedition 352, analytical conditions and detection limits*

Analyzed elements	Filter Position	Detection Limit * (ppm)
Sr	Main	3
Rb	Main	2
Zn	Main	8
Cu	Main	15
Fe	Main	30
Mn	Main	25
Cr	Main/Light	25
V	Main/Light	15
Ti	Main/Light	30
Ca	Light	40
K	Light	75

* As provided by the manufacturer

Table 3: Long-term reproducibility of the shipboard Fisher Niton GOLDD+ XL3t portable XRF instrument

	TiO2 (wt%)	Fe2O3 (wt%)	CaO (wt%)	K2O (wt%)	Zr (ppm)	Sr (ppm)	Rb (ppm)	Zn (ppm)	Cu (ppm)	Mn (ppm)	Cr (ppm)	V (ppm)
BHVO-2 (n =35; 18 Aug - 22 Sept, 2014)	2.65	9.79	10.74	0.56	167	389	9	105	142	1367	221	397
Standard deviation:	0.03	0.05	0.13	0.01	1	2	0.5	2	4	21	6	13
RSD (%):	1.1	0.5	1.2	1.8	0.8	0.5	5.2	2.3	2.6	1.5	2.8	3.2
Accuracy (%):	-2.9	-25.1*	-6.2	6.7	-3	-1.8	-6.3	1.9	10.8	3.7	-26.7*	20.2*
BHVO-2 preferred values:	2.73	12.25	11.4	0.52	172	396	9.11	103	127	1317	280	317

* See discussion in text re: accuracy of Fe, V, and Cr determinations.

Table 4: pXRF Reproducibility and accuracy on rock surfaces

Sample 1092-20	pXRF	2 σ Standard deviation (n = 10)	Coefficient of variation (%)	Variation from reported values (%)	1092-20 values (Reagan et al., 2010)
Major element oxide (wt%):					
TiO_2	1.03	0.04	4	-0.39	1.03
Fe_2O_{3*}	10.72	0.17	1.59	-10.77	12.02
CaO	11.35	0.31	2.72	-8.21	12.36
K_2O	0.24	0.04	16.95	24.37	0.19
Trace element (ppm):					
Sr	68.33	2.25	3.29	-0.54	68.7
Rb	4.04	0.88	21.66	3.7	3.9
Zn	105.24	5.41	5.14	-	-
Cu	179.71	15.36	8.55	-	-
Cr*	225.09	14.04	6.24	-21.02	285
Zr	54.84	2.12	3.86	-4.29	57.3

* Sources of Fe and Cr variation from accepted values are as discussed in the text.